Computational Studies of Pentlandite Mineral: Structural and Dynamical Properties Probed by Molecular Dynamics

M A Mehlape[1], S P Kgalema and P E Ngoepe
Materials Modelling Centre, School of Physical and Mineral Sciences, University of Limpopo, South Africa, Private Bag, X1106, SOVENGA, 0727

E-mail: mofuti.mehlape@ul.ac.za

Abstract. Pentlandite is a major precious metals-bearing mineral and plays a very important role in mining. Precious metal ores co-exists with base metals either as solid-solution and intergrowths, hence rendering its detailed understanding important for efficient extraction of these precious metals. In order to extract the precious metals from the ores effectively it is necessary to study and understand structural and physical properties, of pentlanidte mineral in detail. This work relates to problems in applied areas such as mineralogy, geophysics and geochemistry, whereby phase transition is modified by impurities, so there is the additional concern of the effect of temperature. Computational modelling technique, molecular dynamics (MD) is applied to investigate structural and physical properties of nickel rich pentlandite ($Fe_4Ni_5S_8$). Radial distribution functions (RDFs) and mean square displacement (MSD) are used to establish the effect of temperature on the pentlandite mineral. The MD results are found to compare well with the experimental results.

1. Introduction

The Bushveld Complex has the largest concentration of platinum group elements (PGEs) and these are ruthenium (Ru), rhodium (Rh), palladium (Pd), osmium (Os), iridium (Ir), and platinum (Pt) [1]. Pentlandite minerals are known to host such precious metals, either as solid solutions or as intergrowths [2] and in order to achieve high recoveries of such metals it is necessary to float pentlandites efficiently, particularly in reefs that are less explored, such as the platreef. These PGEs exist in different structures and they could form pentlandite structure ($Fe_4Ni_5S_8$), which makes them significant sulphide minerals. Owing to their high concentration in the Bushveld Complex, it draws much attention in investigating their structure and dynamic properties. In order to extract the precious metals from the ores effectively it is necessary to study, and understand structural and dynamical properties of pentlandites in detail. Notwithstanding their significance in mineralogy, experimental studies on pentlandites are not as abundant as those of pyrites and metal oxide minerals. Moreover, computational modelling investigations probed by molecular dynamics (MD) simulations are also very scarce. There is a need to choose appropriate interatomic potentials for the MD simulation, which might be impossible to get readily available potentials for the material at hand from literature. Here, we present a new set of interatomic potentials for MD simulations of pentlandite ($Fe_4Ni_5S_8$) mineral. The derived interatomic potentials of $Fe_4Ni_5S_8$ were validated by the accurate determination of structure and elastic constants. Furthermore, the potential model yields a melting temperature that is close to the experimental value.

[1] To whom any correspondence should be addressed.

1.1. Pentlandite, $(FeNi)_9S_8$ structure

Pentlandite ($(Fe,Ni)_9S_8$) has a space group of *Fm3m* symmetry and a chemical formula of M_9S_8 (M is a metal). The cation sites may be occupied by Fe and Ni. The structure consists of approximately close-packed alternating layers of sulphur and metal atoms. The cations are distributed across 32 tetrahedral sites in a cube cluster arrangement, each bonded to 4 sulphur anions, and 4 octahedral sites joining the

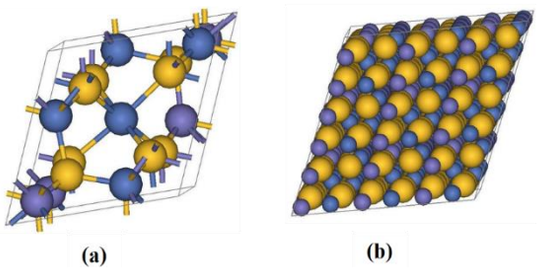

Figure 1. Snapshots of (a) Primitive Unit Cell of $Fe_4Ni_5S_8$ and (b) The initial configuration of a 3x3x3 supercell of $Fe_4Ni_5S_8$ used in the MD calculations, where yellow spheres represent Sulphur, blue spheres represent iron and purple spheres represent nickel.

cube clusters, each bonded to 6 sulphur anions. Of the 32 sulphur atoms, 24 occupy 5- coordinate "face capping" sites, capping the faces of the cube clusters, and the remaining 8 sulphur anions occupy 4-coordinate sites "linking" the cube clusters [3]. Figure 1 shows (a) the primitive unit cell and (b) the initial configuration of a 3x3x3 supercell of $Fe_4Ni_5S_8$ constructed using BIOVIA Materials Studio [4].

2. Computational Details

2.1. Molecular dynamics simulations setup

The study is based on atomistic simulation of pentlandite structure ($Fe_4Ni_5S_8$). The atomistic simulation method uses interatomic potential functions to describe the total energy of a system in terms of atomic coordinates. The static energy minimization code, General Utility Lattice Program (GULP) [5] was used to derive interatomic potentials. The molecular dynamics (MD) simulations are performed to calculate the properties of 3x3x3 supercell of $Fe_4Ni_5S_8$ using GULP as implemented in BIOVIA Materials Studio. MD simulation were run for 500 ps and equilibrated for 100 ps. Temperature is controlled by the canonical ensemble (NVT) constant number of particles (N), volume (V), temperature (T). Temperature is controlled by a Nose-Hoover thermostat [6] and the equation of motion were integrated using the Verlet Leapfrog algorithm [7] with a time step of 1 fs. The constant temperature and volume simulations were performed over the temperature range of 300 K to 1500 K with 100 K increments. In this work, we consider the approximation for describing the pentlandite structure ($Fe_4Ni_5S_8$), which is the rigid ion model potential. This is an empirical approach and relies on a set of parameters, which were modified using cobalt pentlandite potentials (Co_9S_8) [8]. The potential models can accurately describe the bulk and surface structure properties, lattice constants, and elastic properties of sulphides [9], oxides [10], and other pentlandite structures [11].

2.2. Representation of interatomic potentials

The MD calculations in this work are based on the Born ionic model [12] of a solid and parameters were derived for short range interactions represented by the Buckingham potential, Morse potential and three body terms.

2.2.1. Buckingham Potential.

In the Buckingham potential, the repulsive term is replaced by an exponential term and potential takes the form:

$$U(r_{ij}) = A_{ij} e^{-r_{ij}/\rho_{ij}} - \frac{C_{ij}}{r_{ij}^6}, \quad (1)$$

where A_{ij} and ρ_{ij} are parameters that represent the ion size and hardness, respectively, while C_{ij} describe the attractive interaction and r_{ij} is the distance between ion i and ion j. The first term is known as the Born-Mayer potential and the attraction term (second term) was later added to form the Buckingham potential. For the cation-anion interactions, the attractive term is ignored due to the very small

contribution of this term to the short-range potential, or, alternatively, the interaction is subsumed into the A and ρ parameters.

2.2.2. Morse Potential.
The Morse potential is used to model the interactions between covalently bonded atoms and has the form:

$$U(r_{ij})=D_{ij}\left(1-e^{(-B_{ij}(r_{ij}-r_0))}\right)^2-D_{ij}, \quad (2)$$

where D_{ij} is the bond dissociation energy, r_0 is the equilibrium bond distance, and B_{ij} is a function of the slope of the potential energy well. The Coulombic interactions between covalently bonded atoms are often partially or totally ignored as the Morse potential already contains the attractive component of the interaction between neighbours.

2.2.3. Three-Body Potential.
A further component of the interactions of covalent species is the bond-bending term, which is added to take into account the energy penalty for deviations from the equilibrium value. Hence, this potential describes the directionality of the bonds and has a simple harmonic form:

$$U(\theta_{ijk})=\frac{1}{2}k_{ijk}(\theta_{ijk}-\theta_0)^2, \quad (3)$$

where k_{ijk} is the three-body force constant, θ_0 is equilibrium angle and θ_{ijk} is the angle between two interatomic vectors $i-j$ and $i-k$. The interatomic potentials used for this study are given in Table 1.

Table 1. Interatomic potential parameters for the pentlandite $Fe_4Ni_5S_8$ as derived in the present study.

Interatomic potential parameters			
	Charges		
Ions			
Nickel (Ni)	0.40		
Iron (Fe)	0.40		
Sulphur (S)	-0.45		
Buckingham potential			
S-S	1130.533064	0.184528	20.0
Morse potential	$A_{ij}(eV)$	ρ_{ij}(Å)	$C_{ij}(eV$Å$)$
Fe-S	3.0	1.47	2.20
Ni-S	3.0	1.90	2.20
Three body potential	$D_{ij}(eV)$		$\alpha_{ij}(eV)$
Fe-S-S	2.82	109.503	r_0(Å)
S-Fe-Fe	0.80	109.503	
S-Ni-Ni	2.30	109.503	
Ni-S-S	1.72	109.503	$\theta_0(°)$
S-Fe-Ni	1.60	109.503	
	$k(eVrad^{-2})$		

3.1. Results and discussion
In this section, the results from both the bulk properties and molecular dynamics (MD) simulations of $Fe_4Ni_5S_8$ are presented. In Section 3.1, the interatomic potentials are validated by calculating the bulk properties, which includes lattice constants, bond lengths and elastic constants. In section 3.2, we present MD simulations, which include structural and dynamical properties of $Fe_4Ni_5S_8$.

3.1. Bulk Properties
The derived interatomic potentials given in Table 1 have been applied successfully to $Fe_4Ni_5S_8$. The potential models are developed to simplify the complexity of the quantum mechanical computations. The accuracy of the derived interatomic potentials was first checked by comparing the known experimental and calculated data. To validate our potential models we start by showing the properties

that where obtained from our derived potentials i.e., lattice constants, bond lengths and elastic constants. The properties calculated from the derived potential model are in good agreement with those from DFT calculations. The lattice constants, bond lengths and elastic constants of $Fe_4Ni_5S_8$ are listed in Table 2.

Table 2. Lattice constants, bond lengths and elastic constants of $Fe_4Ni_5S_8$

	Potential Model	**Density Functional Theory (DFT)**
Lattice Parameter (Å)		
a	7.015	7.012
b	6.855	7.039
c	6.976	7.024
Volume ($Å^3$)	238.236	237.358
Density of Cell (g/cm^3)	5.390	5.410
Bond Length (Å)		
Fe-S	2.11	2.22
Ni-S	2.09	2.20
Fe-Fe	2.45	2.50
Ni-Ni	2.49	2.53
S-S	3.27	3.22
Elastic Constant (GPa)		
C_{11}	205.50	207.8
C_{12}	100.72	102.38
C_{44}	49.40	47.07
Bulk Modulus (GPa)	131.35	137.31

3.2. Structural and dynamical properties

RDF is an important parameter to describe the structural characteristics of solid, amorphous and liquid states [13]. It defines the probability of finding an atom in a distance ranging from r to r+dr (dr is the step of calculation) and is expressed as:

$$g(r)=\frac{V\sum_{i=1}^{N_i} n_i(r)}{N^2 4\pi r^2 dr}, \quad (4)$$

where V and N are the volume and total number of atoms of the system, N_i is the number of atoms around i^{th} atom and $n_i(r)$ is the corresponding atom number in the sphere shell ranging from r to r + dr at the radius r. Figure 2 shows the radial distribution functions (RDFs) for the $Fe_4Ni_5S_8$ supercell at various temperatures, from 300 K to 1500 K. From the radial distribution function plots we observe that at lower temperatures of 300 K there are several sharp peaks, implying a well-ordered structure. However, as we increase the temperature the peaks become broader and their number decreases, showing that the structure is experiencing the phase transition from a solid phase to a liquid phase. This happens mainly at the temperature of 1300 K, wherein the arrangement of atoms is fading and the peaks are broad, which corresponds to the structure melting. This agree with the experimental melting temperature of $Fe_4Ni_5S_8$, which is approximately 1255 K [14]. Figure 3 shows the snapshots for 3x3x3 supercell structure of $Fe_4Ni_5S_8$ simulated at various temperatures. From the pictures we observe that there is a phase transition from a lower temperature to a higher temperature. At temperatures 300 K to 900 K, the structure is still well maintained showing crystallinity. However, as we increase the temperature to 1300 K, we observe that the structure loses its crystallinity, as the regular arrangement of atoms disappears. It can be seen that the arrangement of atoms has completely disappeared at a temperature of 1300 K, which is in agreement with the variation trend of the RDF results described above.

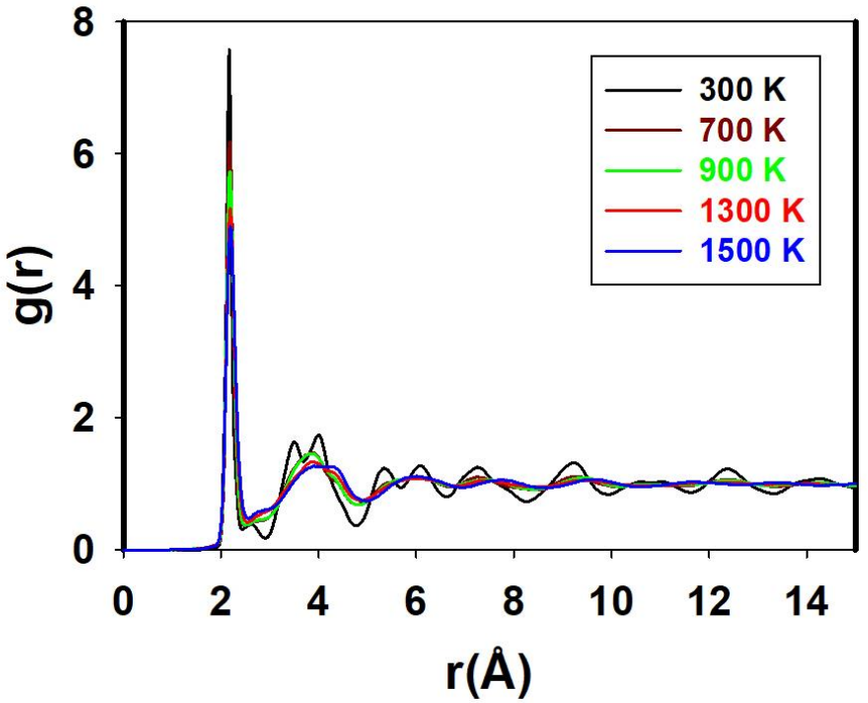

Figure 2. The radial distribution functions (RDFs) of $Fe_4Ni_5S_8$ at various temperatures

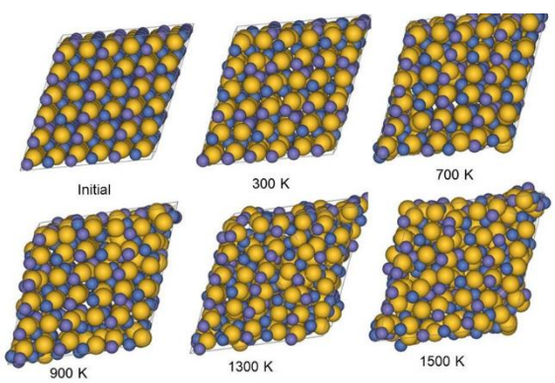

Figure 3. Structural changes of $Fe_4Ni_5S_8$ structure after MD simulations at various temperatures.

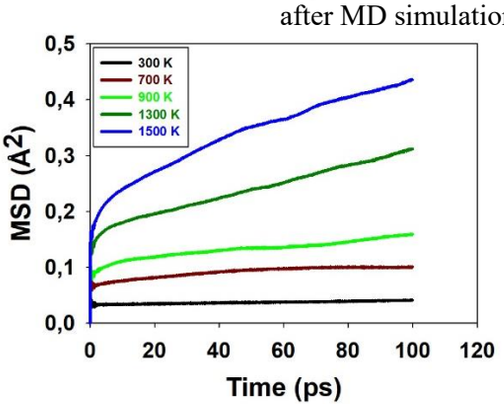

Figure 4. The variation of MSD of $Fe_4Ni_5S_8$ with time at various temperatures.

 ISBN: 978-0-620-97693-0

Mean square displacement (MSD) refers to the square of the average displacement of particles in a certain period of time [15]. MSD in MD simulations show that the position and the direction of the motion of particles keep changing, especially at high temperatures. Figure 4 shows the total MSD as a function of time at different temperatures from 300 K to 1500 K. From the MSD of $Fe_4Ni_5S_8$, at lower temperatures of 300 K to 900 K, it predicts that the mobility of atoms within the structure is less. As temperature is increased to 1300 K and 1500 K the mobility of atoms in the pentlandite structure increases. At a simulation time of around 100 picoseconds, the mobility of atoms is more at higher temperatures, which is between 1300 K and 1500 K. The same temperature range was observed through the RDFs in Figure 2. Figure 4, demonstrate that after initial diffusion for a period of time, the ions quickly reached the stable stage and then maintained a relatively stable diffusion level. A linear relationship is observed between MSD and simulation time.

4. onclusion

Molecular dynamics simulations were performed with the aim of investigating the dynamic and structural properties of pentlandite structure. The melting of the structure was observed through the radial distribution function (RDFs). At low temperature (300 K) the RDFs have many and sharp peaks, however, at higher temperature (1300 K) the RDFs curve are relatively smooth and does not exhibit any defined peaks, indicative of structural change from solid to liquid phase. Furthermore, through the mean-squared displacement (MSD), the results show that MSD increases with temperature and atoms are able to move more at high temperature. MSD increases with time in all investigated temperatures and there is a linear relationship between MSD and simulation time.

Acknowledgements

The computations were performed at the Materials Modelling Centre (MMC), University of Limpopo and at the Centre for High Performance Computing (CHPC), Cape Town. We also acknowledge the National Research Foundation (NRF) for funding.

References

[1] O'Connor T C and Shacklenton N J 2013 *Platin. Met. Rev.* **57** 302
[2] Wang Q and Heiskanen K 1990 *Int. J. Miner. Process.* **29** 99
[3] Hoodless R C, Moyes R B and Wells P B 2006 *Catal. Today* **114** 377
[4] BIOVIA, Materials Studio, (20.1.051), Dassault Systemes, San Diego, 2020
[5] Gale J D 1997 *J. Chem. Soc., Faraday Trans.* **93** 629
[6] Nosé S 1990 *J. Phys.:Condens. Matt*er. **2** 115
[7] Verlet L 1967 *Phys. Rev*. **159**, 98
[8] Mehlape M A 2013 *PhD Thesis*. University of Limpopo
[9] Sithole H M, Ngoepe P E and Wright K 2003 *Phys. Chem. Miner*. **30** 615
[10] Maphanga R R, Ngoepe P E and Parker S C 2009 *Surf. Sci.* **603** 3184
[11] Mehlape M A, Ngoepe P E and Parker S C 2013 Proceedings of SAIP 98-103 Available online at http://events.saip.org.za
[12] Born M and Huang K. 1954 *Dynamical Theory of Crystal Lattices 1st edition*. Oxford: University Press
[13] Zhanga X, Lia B, Liu H X, Zhao G H, Yanga Q L, Chenga X M, Wong C H, Zhang Y M and Lime C W J 2019 *Appl. Surf. Sci.* **465** 871
[14] Kitakaze A and Sugaki A 2004 *Can. Mineral.*, **42** 17
[15] Wang G, Cui Y, Li X, Yang S, Zhao J, Tang H and Li X 2020 *Minerals*, **10** 149